The protoplanetary disk of FT Tauri: multi-wavelength data analysis and modeling

Garufi et al., arXiv:1405.7692

・FT Tauという星+円盤のSEDを文献から作成

・合うモデルを輻射輸送込みで計算(モデル:MCFOST and ProDiMo)

・観測結果の解釈

  中心星: 0.3Msun, 0.35Lsun, 年齢 1.6Myr

  M型星にしては高い降着率(3.1・10^{-8} Msun/yr)

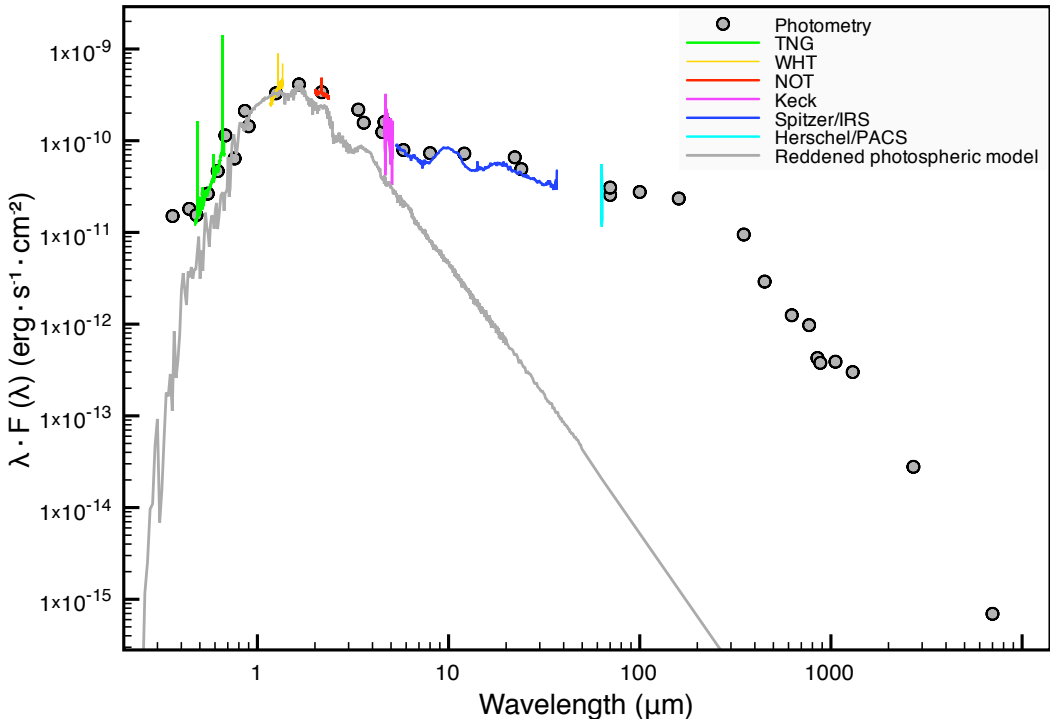 それなりに重い円盤(0.02Msun)←中心星の0.06倍

  円盤内縁が非常に小さい(0.05AU)

  ←COのline幅から導出。inclinationは輻射輸送モデルから持ってくる

  小さいsilicate (0.1μm)は円盤表面にまだ存在

  ←silicate feature at 10 μmが見えるから

Parameter	Symbol	Comments	Value
Stellar luminosity	L_*	Derived from observations	$0.35\ L_\odot$
Stellar mass	M_*	”	$0.3\ M_\odot$
Stellar radius	R_*	”	$1.7\ R_\odot$
Effective temperature	T_{eff}	”	3400 K
Distance	d	”	140 pc
Slope of UV excess distribution	p_{UV}	Fixed in MCFOST	2.0
Slope of grain size distribution	a_{pow}	”	3.5
Dust mass density	ρ_{d}	”	$3.5\ \mathrm{g\ cm}^{-3}$
Slope of surface mass density	ϵ	”	-1
Flaring reference radius	R_0	Explored with MCFOST	100 AU
Flaring reference height	H_0	”	12, 14 AU (high/low f_{UV})
Flaring exponent	β	”	1.15
Disk inner radius	R_{in}	”	0.09, 0.05 AU (high/low f_{UV})
Minimum dust grain size	a_{min}	”	0.05, 0.1 μm (high/low f_{UV})
Maximum dust grain size	a_{max}	”	1 cm
Stratification exponent	s_{set}	”	0.2, 0.3 (high/low f_{UV})
Stratification grain dimension	a_{set}	”	0.05, 0.1 μm (high/low f_{UV})
Inclination	i	”	60°
Disk outer radius	R_{out}	”	50, 100, 200 AU
Optical extinction	A_V	Free parameter in MCFOST	1.6
Disk dust mass	M_{d}	”	$9 \cdot 10^{-4}\ M_\odot$
Cosmic Ray Ionization rate	ζ	Fixed in *ProDiMo*	$1.7 \cdot 10^{-17}\ \mathrm{s}^{-1}$
UV excess	f_{UV}	Explored with *ProDiMo*	0.07, 0.025
PAH abundance	f_{PAH}	”	$10^{-2}, 10^{-3}, 10^{-4}$
Disk gas mass	M_{g}	”	$(9, 4.5, 1.8) \cdot 10^{-2}\ M_\odot$

Shadows and cavities in protoplanetary disks: HD163296, HD141569A, and HD150193A in polarized light
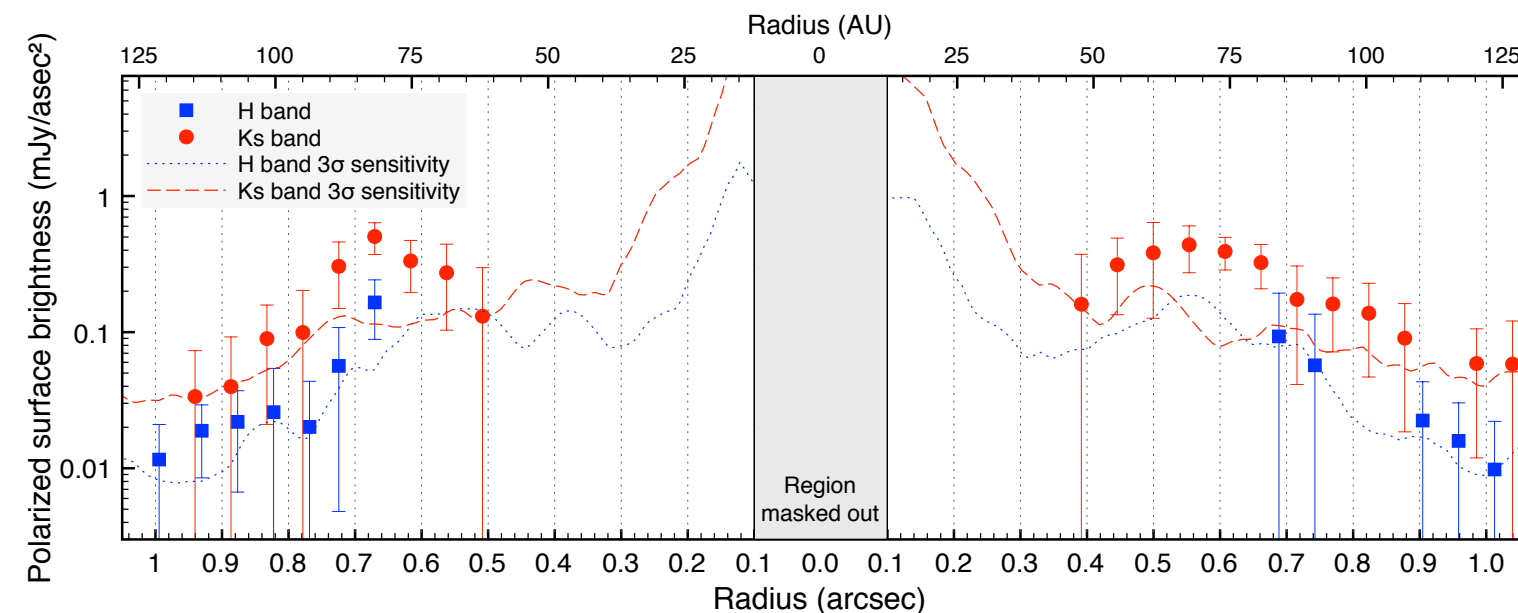
Garufi et al., arXiv:1406.7387

・近赤外の高分解能偏光観測により円盤を観測（VLTのNACOという装置）

・観測天体：HD163296, HD141549A, HD150193A
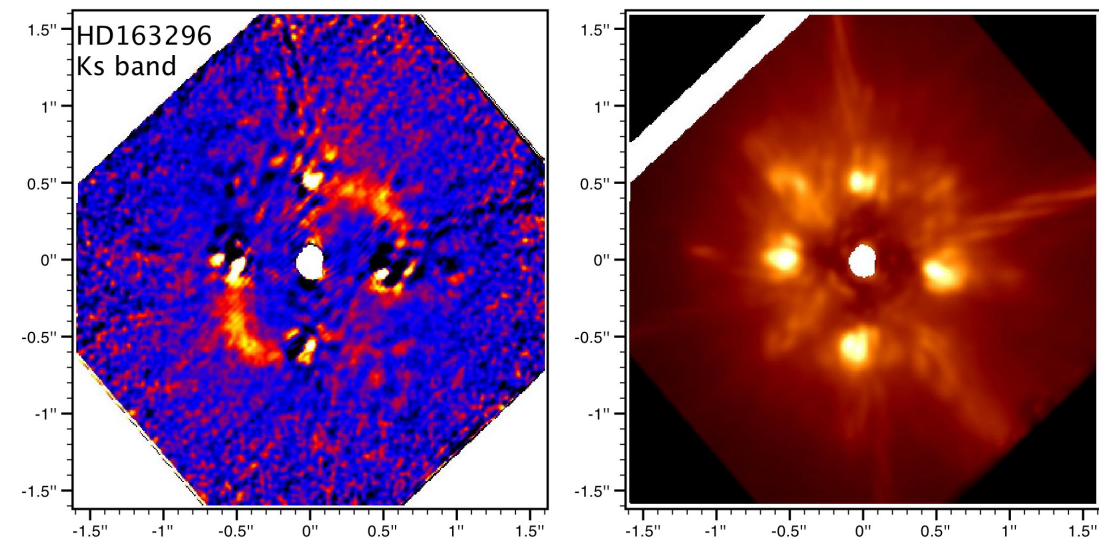
・結果：HD163296ではHとKsの両方で円盤を検出、他２つは受からない

AOの引き残りがたくさん

動径分布はぱっと見0.6"くらいにピークを持つようにみえる

→transitional diskっぽい？？→self-shadowingの議論

【コメント】（外側2"以遠の明るさの変動を円盤内側の変動＋self-shadowing

で議論しているが、本観測からは有益な結論はあまりなさそう…）

動径分布, 赤:Ks, 青:Hバンド

左:偏光, 右: total I (どちらもr^2でスケール)

The masses of young stars: CN as a probe of dynamical masses

Guilloteau et al., arXiv:1406.3805

・中心星の質量を知りたい。COは分子雲などのコンタミが大きいので、ここ

では円盤のCN(1-0)のフィッティングによる中心星質量の導出を提案する。

・サンプルは12天体 (うちT Tauri星が 9個)
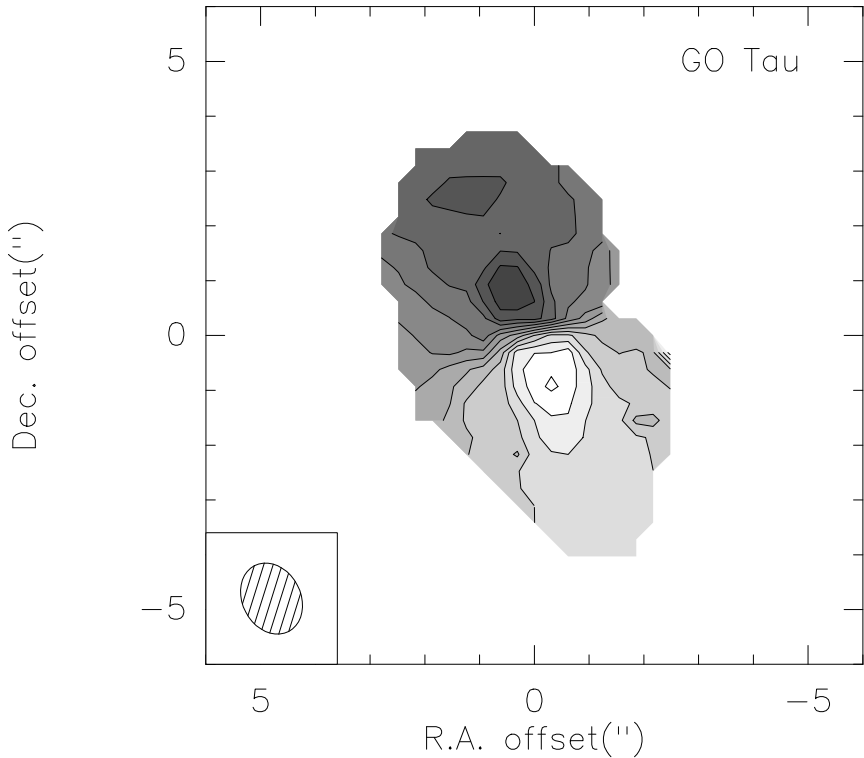
・Kepler回転からのズレはごくわずか v ∝r^(0.5 + 0.005)くらい→星の質量が

正確に決まる

Fig. 3. Velocity gradient for GO Tau. Contour spacing is $0.2\ \mathrm{km\,s^{-1}}$.

Table 4. Disk and Star parameters derived from CN

Source name	V_{100} (km s^{-1})	i (°)	R_{out} AU	M$_*$ ($M_\odot$)	δv
DM Tau	2.31 ± 0.17	-30.9 ± 2.9	641 ± 19	0.60 ± 0.09	0.1 ± 1.5
MWC 480	4.03 ± 0.41	36.3 ± 2.5	539 ± 39	1.83 ± 0.37	-2.2 ± 2.0
LkCa 15	3.11 ± 0.10	47.0 ± 1.3	567 ± 39	1.09 ± 0.07	0.0 ± 2.4
CI Tau	2.67 ± 0.03	51.0 ± 0.9	520 ± 13	0.80 ± 0.02	-2.7 ± 2.0
CY Tau	2.36 ± 0.12	24.0 ± 2.0	295 ± 11	0.63 ± 0.05	1.7 ± 1.7
GO Tau	2.07 ± 0.01	54.5 ± 0.5	587 ± 55	0.48 ± 0.01	4.0 ± 2.0
HV Tau C	3.76 ± 0.10	89.1 ± 3.0	256 ± 51	1.59 ± 0.08	-0.0 ± 2.9
DL Tau	2.83 ± 0.04	44.1 ± 2.6	463 ± 6	0.91 ± 0.02	1.9 ± 1.1
IQ Tau	2.64 ± 0.02	56.3 ± 3.9	225 ± 21	0.79 ± 0.02	-0.3 ± 4.9
DN Tau	2.91 ± 0.25	29.2 ± 3.0	241 ± 7	0.95 ± 0.16	-0.6 ± 1.8
04302+2247	4.18 ± 0.09	58.9 ± 2.1	750 ± 56	1.97 ± 0.08	-0.4 ± 2.3

Notes. δv is the departure from Keplerian rotation: $v(r) \propto r^{-(0.50+0.01\,\delta v)}$.

HR図から出した星の質量との比較

Table 7. Approximate ages (Myr)

#	Star	Evolutionary Tracks			
		BCAH	SDF	Pisa	Dartmouth
3.	IQ Tau	2	3	3	2
5.	DL Tau	3	4	4	3
6.	DM Tau	5	8	5	3.5
7.	CI Tau	1.5	2.5	2.5	1.5
9.	LkCa 15	3	4	4	3
11.	GO Tau	2	4	3	3
13.	GM Aur	2	2	2	1.5

Table 6. Comparison of best Masses with tracks

#	Star	Dynamical Mass	Agreement & Evolutionary Track Mass range			
			BCAH	SDF	Pisa	Dartmouth
3.	IQ Tau	0.79 ± 0.02	F 0.65-0.70	F 0.45-0.70	F 0.48-0.72	P 0.50-0.60
5.	DL Tau	0.91 ± 0.02	E 0.72-0.92	E 0.60-0.92	F 0.62-0.88	F 0.68-0.88
6.	DM Tau	0.53 ± 0.02	E 0.50-0.70	E 0.35-0.59	E 0.43-0.62	E 0.44-0.62
7.	CI Tau	0.80 ± 0.02	E 0.70-0.88	E 0.58-0.90	E 0.60-0.82	E 0.59-0.80
9.	LkCa 15	1.01 ± 0.03	E 0.92-1.30	E 0.95-1.30	E 0.90-1.25	E 0.92-1.30
11.	GO Tau	0.48 ± 0.01	P 0.70-0.92	E 0.45-0.75	F 0.52-0.82	E 0.48-0.70
13.	GM Aur	1.00 ± 0.02	P 1.35-?	P 1.51-?	P 1.30-?	P 1.20-?

Notes. Qualitative agreement: E= Excellent G= Good F= Fair P= Poor

Accretion and Diffusion Timescales in Sheets and Filaments

Heitsch and Hartmann, arXiv:1406.2191

星形成において、subcriticalからどうやってsupercriticalになるか、遷移過程を知りたい。

subcritical状態でも磁力線に沿ってものが降着した場合、そのうちsupercriticalになる

→accretionとdiffusion/gravitational fragmentationのどちらが早いかで決まる

→なのでタイムスケールを調べる

・シートがものを重力で集めるタイムスケール。圧力無視してfree-fallで落ちてくるとすると accretion rateが出る。これでmass-to-flux ratioが $\frac{\Sigma}{B} > \left(\frac{\Sigma}{B}\right)_c \equiv \frac{1}{2\pi G^{1/2}}$ を超えるためには

$$\tau_{acc} = \frac{1}{a}\left(2\left(\frac{B}{2\pi G^{1/2}} - b\right)^{1/2} - \Sigma_0^{1/2}\right). \qquad \Rightarrow \qquad \tau_{acc} \approx (2\pi G \rho_0)^{-1/2}\left(\frac{\Sigma_c}{\Sigma_{acc}}\right)^{1/2},$$

・filamentの場合のaccretionも計算。質量がTomisaka 2013式を超えるまで。

$$m_{rad} = 0.24\frac{BR}{\sqrt{G}} + 1.66\frac{c_s^2}{G},$$

これらのタイムスケールを、ambipolar diffusionなどのタイムスケールと比べる

シートの時のもっとも短いタイムスケールを表した図　　　◇はKudoh & Basu 2011
gravitational fragmentation, **accretion**, **laminar ambipolar diffusion**
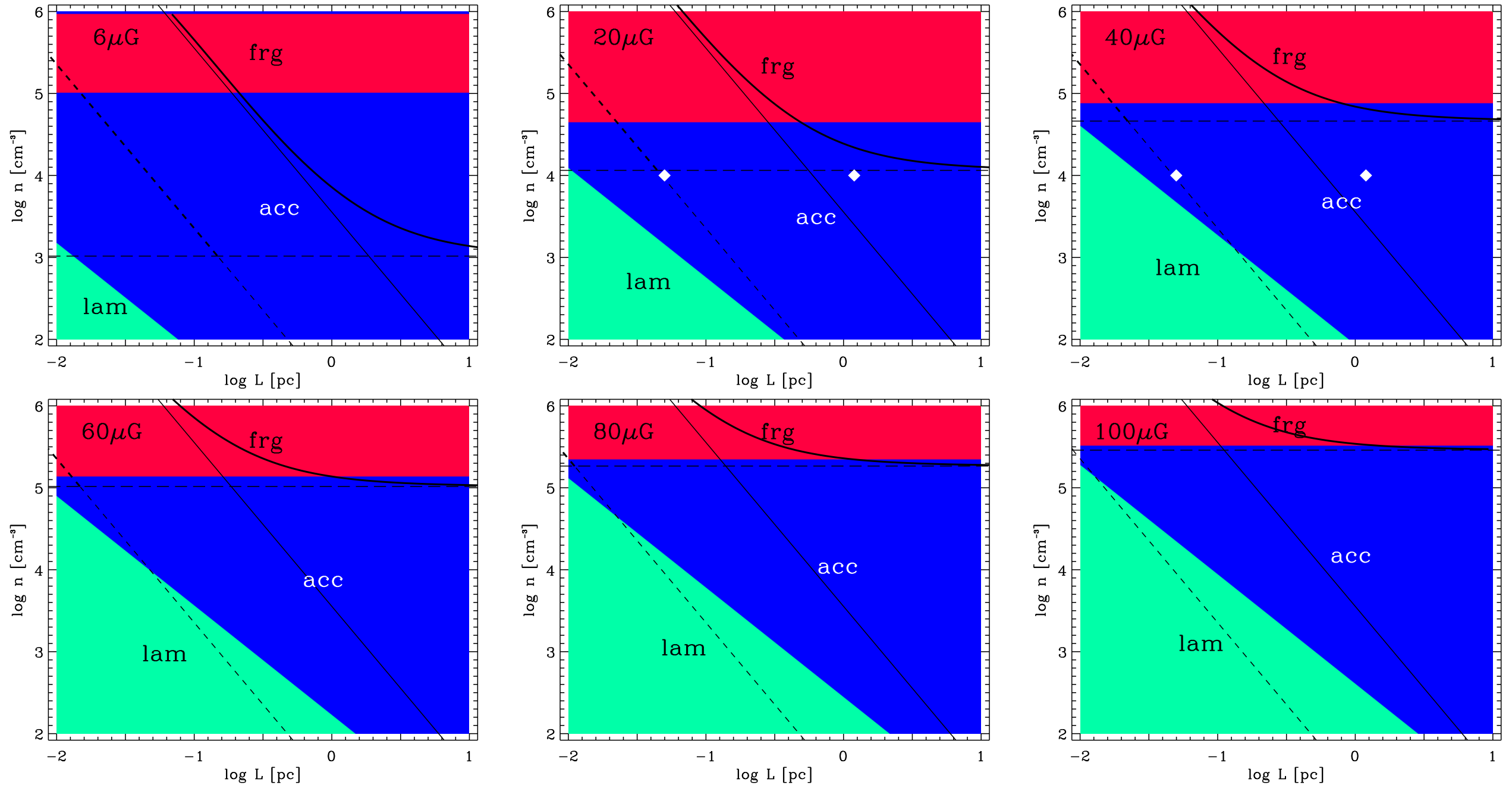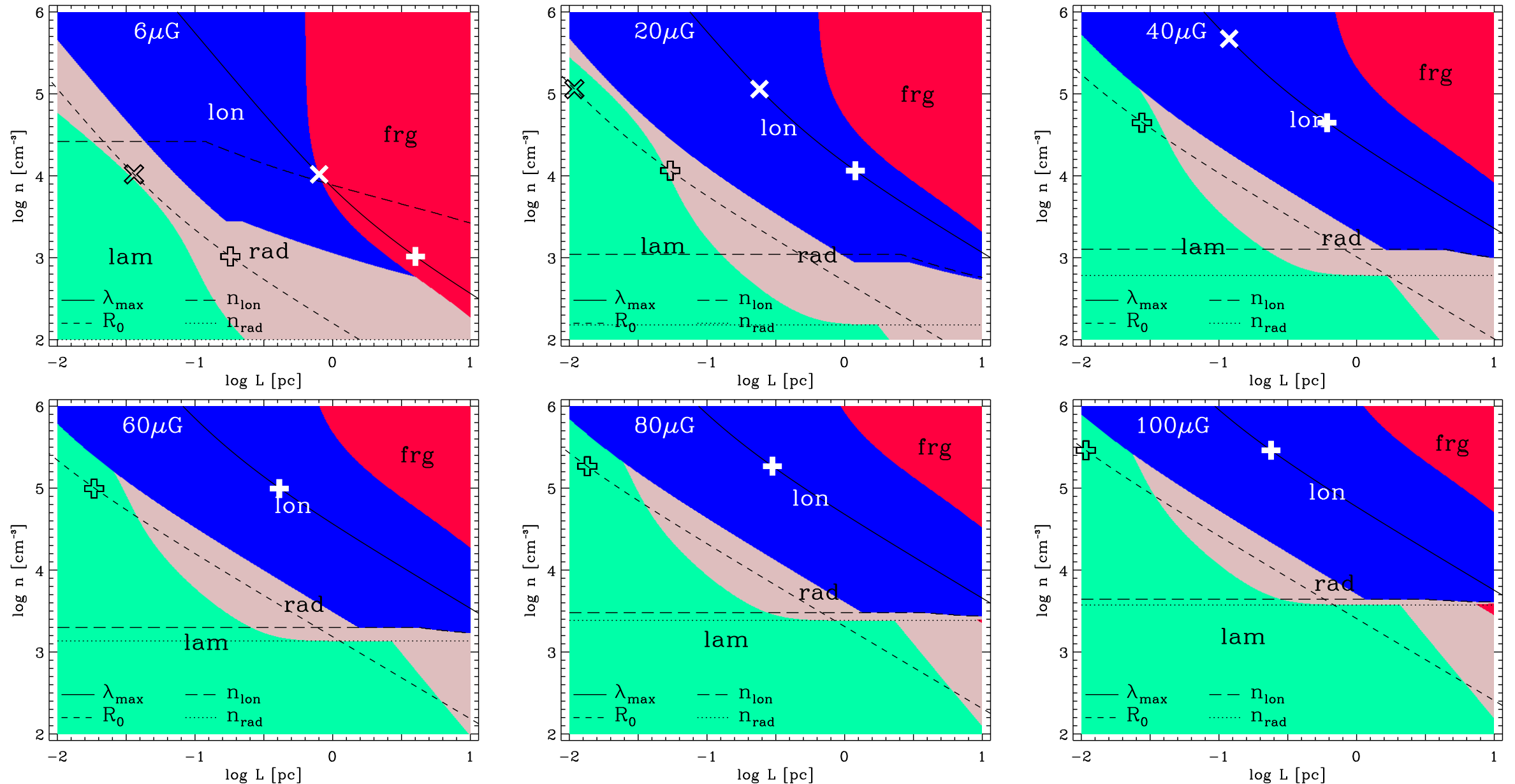
Figure 3. Map of the shortest timescales in the length scale-density plane for a sheet. For a given combination of (L, n), all relevant timescales are compared, and the regime of the shortest timescale is color-coded as blue for accretion (*acc*), red for gravitational fragmentation (*frg*), and light green for laminar ambipolar diffusion (*lam*). The solid curved line shows the wavelength of the most unstable (magnetized) mode, λ_{max}, against the sheet's central density (Larson 1985), the solid straight line is the corresponding hydrodynamical mode, and the dashed line shows the sheet's scaleheight against central density. Criticality is indicated by the horizontal, long-dashed line (eq. 22). White diamonds show the initial conditions for models run by Kudoh & Basu (2011, see Sec.4.1.2).

フィラメント

gravitational fragmentation, accretion(磁場に沿った方向), accretion(radial),

laminar ambipolar diffusion

Figure 5. Map of the shortest timescales in the lengthscale-density plane, for a filament. For a given combination of (L, n), all relevant timescales are compared, and the regime is color-coded as longitudinal criticality (blue, *lon*), radial criticality (pink, *rad*), gravitational fragmentation (frg, *red*), and laminar ambipolar diffusion (light green, *lam*). The solid line shows the wavelength of the most unstable mode, λ_{max} (Nagasawa 1987) against the filament density, and the dashed line shows the filament's core-radius R_0 (eq. 23). Longitudinal criticality is indicated by the long-dashed line (eq. 21), and radial criticality by the dotted line. Symbols denote the evolution of the two filament accretion models shown in Fig. 2.

ambipolar diffusionはシートやフィラメントの成長に効かない。

それより先にものが accretion して supercritical になる。

＊ただし、乱流拡散がシートでは強磁場の場合(20μG以上)重要。フィラメントでは乱流拡散は小スケールしか効かない

結論：アクリーションが重要。

Two Extreme Young Objects in Barnard 1-b

Hirano and Liu, arXiv:1406.0068

B1-bというコアは4.7Msun、0.12×0.07pc (野辺山45mのH^{13}CO(1-0)より,左下図)

B1-bは２つの点源からなる(B1-bNとB1-bS, 3.3mm連続波より, 右下図)

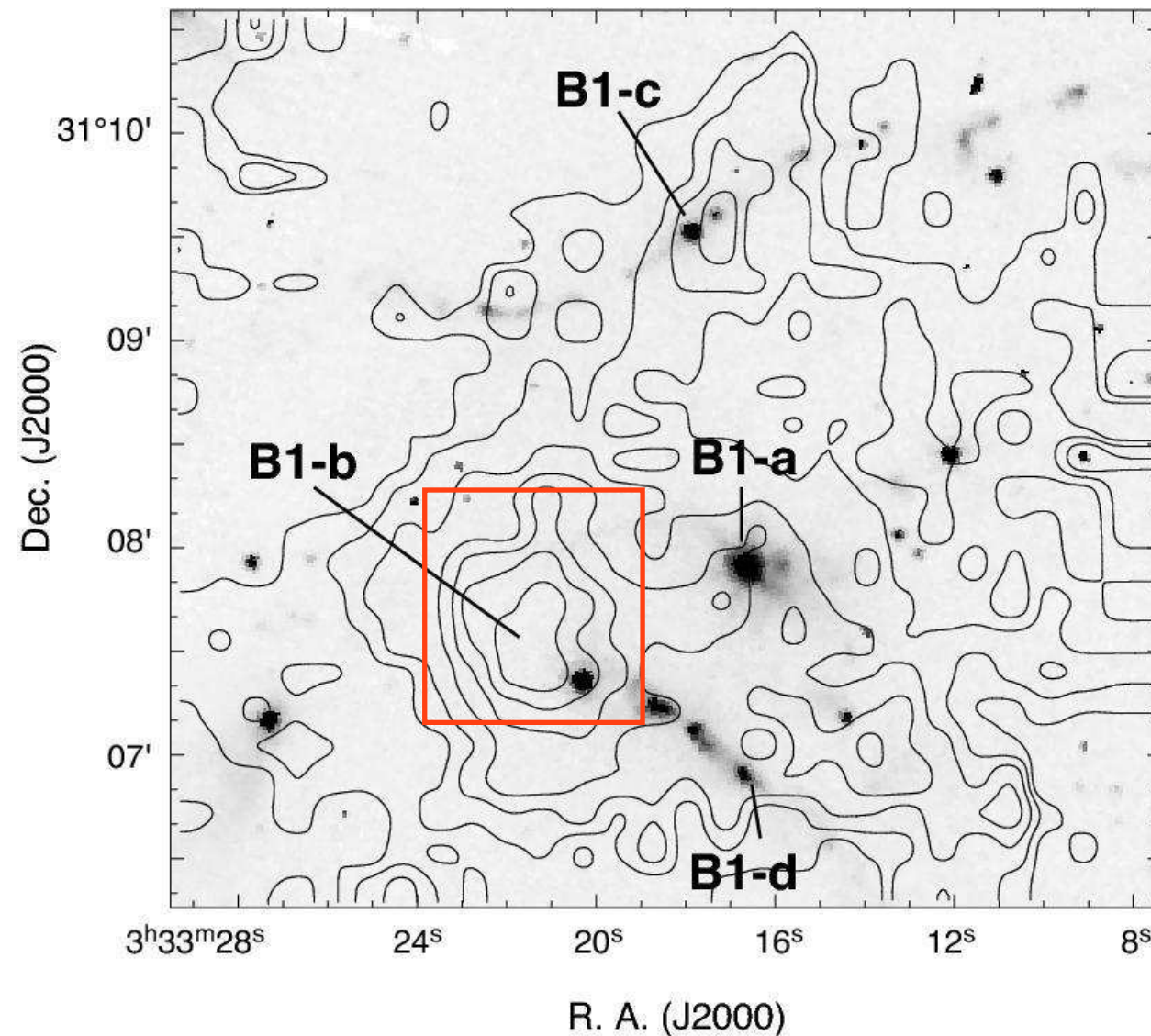COでoutflow確認。3-5km/s for B1-bN, 7-8km/s for B1-bS

Fig. 1.— Integrated H^{13}CO$^+$ (J=1-0) emission from B1 (contours) on top of the Spitzer IRAC band 2 (4.5 μm) image (grey scale). The velocity range of the H^{13}CO$^+$ map is from $V_{LSR} = 5.0$ to 8.0 km s^{-1}. The contours start from 0.67 K km s^{-1} (3 σ) with an interval of 0.44 K km s^{-1} (2 σ).
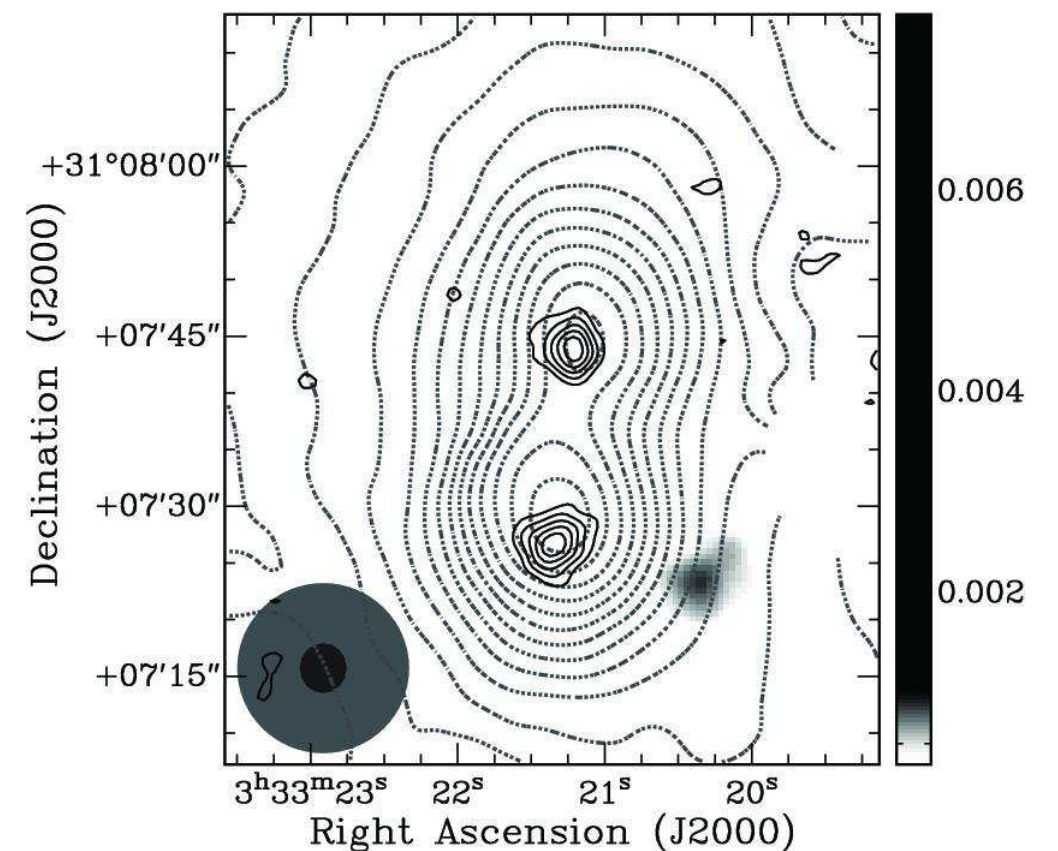

Fig. 4.— 850 μm (dot contours) and 3.3 mm (solid contours) continuum maps of the B1-b region on top of the Spitzer MIPS 24 μm image (grey scale). The 3.3 mm continuum has been applied for the primary beam correction. The gray-filled and black-filled circles in the lower-left courner are the beams of 850 μm and 3.3 mm, respectively. The contours are drawn every 0.08 Jy/beam (3 σ) for 850 μm and 3.4 mJy/beam (2.5 σ) for 3.3 mm.
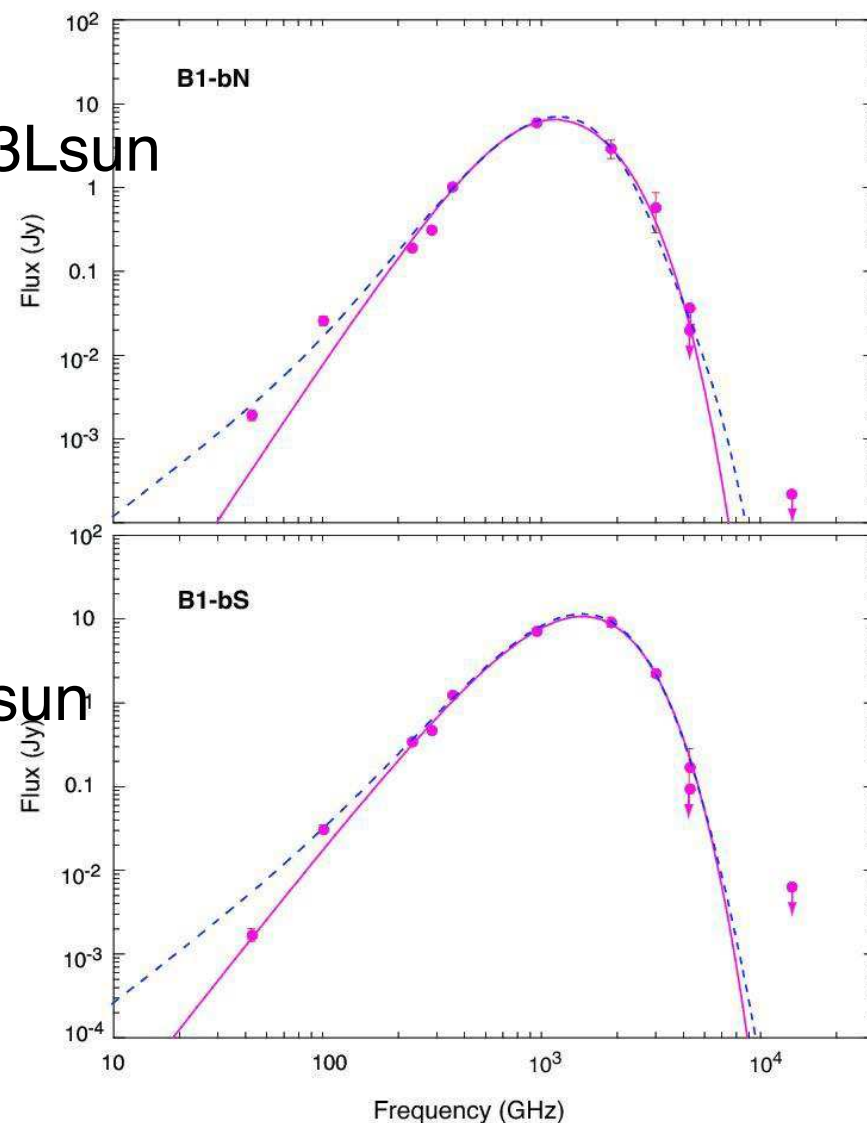
このうちB1-bNはファーストコアだと思われる
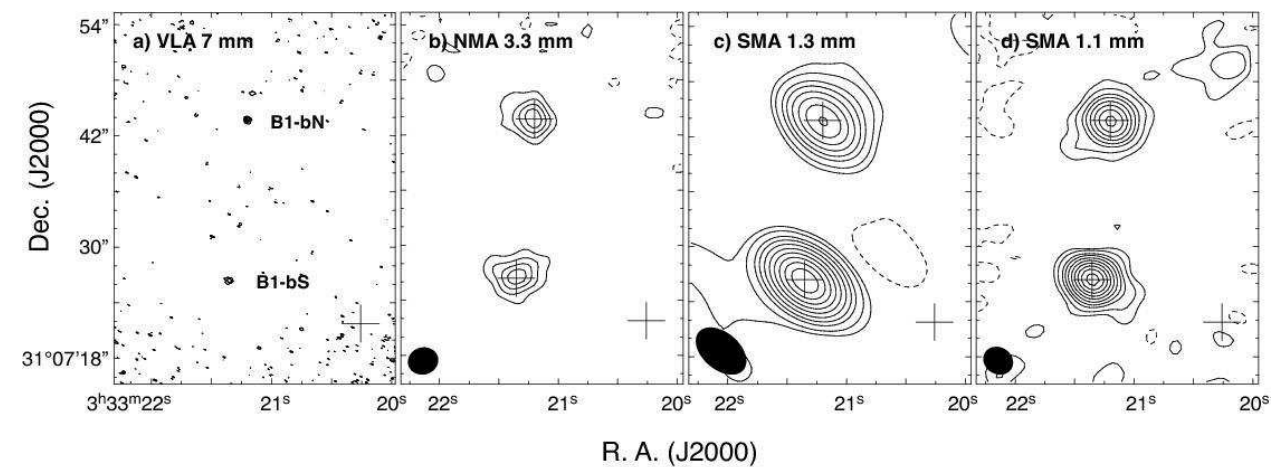
B1-bN

L_{int}<0.01-0.03Lsun

Fig. 5.— Maps of the continuum emission at millimeter wavebands. All the maps are corrected for the primary beam response. (a) 7 mm continuum map observed with the VLA. The contours are drawn every 3 σ. The cross denotes the position of B1-bW. (b) 3.3 mm continuum map observed with the NMA. The contours are drawn every 3 σ. The crosses indicate the positions of B1-bN, B1-bS, and B1-bW. (c) 1.3 mm continuum map observed with the SMA. The contours start at 3σ and are drawn at 6, 12, 18, 27, 39, 54, 72, 93, 117, and 144σ. (d) 1.1 mm continuum map observed with the SMA. The contours start at 3σ and are drawn at 6, 12, 18, 27, 39, 54, 72, 93, and 117σ.

B1-bS

L_{int}=0.1-0.2Lsun

・それぞれmm波でcompactな天体

→diskの起源か？

L_{bol}~0.14-0.31Lsun

Fig. 7.— Spectral energy distributions of B1-bN (upper panel) and B1-bS (lower panel). The data are from Spitzer MIPS (24 and 70 μm), CSO SHARC (350 μm), JCMT SCUBA (850 μm), SMA (1.1 mm and 1.3 mm), NMA (3.3 mm), and VLA (7 mm). Arrows mark the upper limits. The solid red curves are the single-component greybody fits with $T_{dust} \approx$ 16 K and $\beta = 2.0$ for B1-bN and with $T_{dust} \approx$ 18 K and $\beta = 1.3$ for B1-bS. The dashed blue curves are the results of the two component model with a compact blackbody component and an extended greybody component. The parameters of the two component models are $T_{dust}(ext) \approx 11$ K, $\beta(ext) = 2.0$, and $T_{dust}(cmp) = 23$ K for B1-bN, and $T_{dust}(ext) \approx 16$ K, $\beta(ext) = 1.5$, and $T_{dust}(cmp) \approx 24$ K for B1-bS.